Development of Functional Polymer Gel Electrolytes and Their Application in Next-Generation Lithium Secondary Batteries

Ryota Tamate[1,2]*

[1]Research Center for Macromolecules & Biomaterials, National Institute for Materials Science, 1-2-1 Sengen, Tsukuba, 305-0047, Japan

[2]PRESTO, JST, 7 Gobancho, Chiyoda-ku, Tokyo 102-0076, Japan

E-mail: TAMATE.Ryota@nims.go.jp

Running Head: Functional Polymer Gel Electrolytes

Abstract

Owing to the digital revolution and growing emphasis on sustainability, the demand for innovative electrochemical devices, such as flexible and wearable sensors, energy-harvesting devices, and high-capacity secondary batteries, has been increasing. Alongside this, various high-performance gel electrolytes with excellent mechanical and electrochemical properties have been developed. This focus review presents our recent research on enhancing the mechanical properties of gel electrolytes and their application in lithium secondary batteries. It discusses the efforts made to achieve self-healing ion gels, which utilize ionic liquids as the electrolyte solutions. Additionally, the review covers the application of functional gel electrolytes in next-generation lithium secondary batteries. It focuses particularly on improving the cycling performance of lithium metal anodes, which are considered the very promising anode material. Moreover, the future prospects of functional polymer gel electrolytes have been discussed in this review.

Keywords: gel electrolytes/ion gels/self-healing/toughness/lithium secondary batteries/lithium metal

1. Introduction

Gel electrolytes are soft materials comprising a polymer network swollen with an ion-conductive electrolyte solution. They can provide stability and robustness by becoming quasi-solid while maintaining the electrochemical properties of the electrolyte. Gel electrolytes have attracted significant attention for applications in various electrochemical devices, including capacitors, secondary batteries, sensors, and actuators.[1-5] Recently, there has been a growing demand for innovative electrochemical devices, such as flexible and wearable sensors, energy-harvesting devices that support the Internet of Things (IoT) and digital innovation, and very high-capacity secondary batteries for widespread electric vehicle use. For application in flexible and wearable devices, such as strain sensors, actuators, and flexible batteries, high durability against daily deformation is required. Therefore, gel electrolytes with high mechanical strength and self-healing properties against mechanical damage have attracted significant attention.[6-12] These materials must also exhibit stability in various environments. Many studies have focused on the functionalization of "ion gel (ionogel) electrolytes," which are gel electrolytes swollen with ionic liquids (ILs). These ILs, which are room temperature molten salts, offer promising physicochemical properties, including nonvolatility, nonflammability, and high thermal and chemical stability.[13-17] Section 2 of this review discusses our recent studies on the fabrication of self-healing ion-gel electrolytes using different chemical and physical approaches. Recently, mechanically functional gel electrolytes have become a promising method for improving the cycling performance of next-generation high-capacity negative electrodes, such as lithium (Li) metal and silicon anodes. These electrodes experience significant morphological changes during the charge–discharge processes. In Section 3, we discuss the design of tough gel electrolytes to improve the cycling performance of Li metal anodes, which are considered the very promising anode material owing to their high theoretical capacity and low working potential.

In these functional gel electrolytes, competitive interactions between the electrolyte and polymer significantly affect not only the electrochemical properties but also the mechanical properties. Optimization of these interactions is crucial for achieving the desired physical properties. The future prospects for the implementation of functional gel electrolytes into various applications are also discussed in this review.

2. Self-healing gel electrolytes based on ILs

As electrolytes in electrochemical devices, ILs have several advantages, such as high ionic conductivity, nonflammability, nonvolatility, and thermal/electrochemical stability. Gel electrolytes using ILs as electrolyte solutions are called "ion gels or ionogels," and various functional ion gels have been actively studied over the past several decades.[18-23] Compared to conventional gel electrolytes using aqueous or organic electrolyte solutions, ion gels offer promising properties for next-generation electrochemical devices owing to the intrinsic properties of ILs. However, a significant challenge in their implementation in flexible and wearable devices is achieving sufficient mechanical strength while preserving the excellent physicochemical properties of ILs. Self-healing is one of the most promising methods for enhancing the mechanical properties of polymeric materials. Self-healing polymeric materials achieve unprecedented durability through spontaneous repairing of mechanical damages.[24-29] In this section, we outline our recent work on designing self-healing ion gels using chemical and physical approaches.

2.1 Self-healing ion gels achieved through chemical approaches

Studies on self-healing ion gels based on supramolecular chemistry and dynamic covalent chemistry are increasing annually.[30-39] In self-healing polymeric materials, balancing self-healing properties and with mechanical strength is a key challenge for practical applications. We developed an ion gel that combines self-standing ability, mechanical strength, and rapid self-healing properties by utilizing multiple hydrogen bonds and the nanophase-separated structure of block copolymers (**Figure 1a**).[40] The ion gel was composed of an aprotic IL, 1-ethyl-3-methylimidazolium bis(trifluoromethanesulfonyl)imide ([C_2mim][TFSI]), and a diblock copolymer. The diblock copolymer consisted of a polystyrene (PS) block, which was incompatible with the IL, and a poly(*N*, *N*-dimethylacrylamide-*r*-acrylic acid) (P(DMAAm-*r*-AAc)) block, which exhibited hydrogen-bonding ability (PS-*b*-P(DMAAm-*r*-AAc)). The DMAAm and AAc units in the P(DMAAm-*r*-AAc) block acted as hydrogen bond acceptor and donor, respectively. This diblock copolymer forms a micelle structure because the PS block, which is immiscible with [C_2mim][TFSI], aggregates in the IL, while the P(DMAAm-*r*-AAc) block, which is miscible with the IL, acts as an outer layer surrounding the aggregated PS block. As a result, a percolated network was formed in the IL owing to multiple hydrogen bonds between the jammed block copolymer micelles. The ion gel formed through the introduction of the jammed micellar network exhibited significantly enhanced self-standing ability and mechanical strength compared to that formed solely from the hydrogen-bonded P(DMAAm-*r*-AAc) copolymers (**Figure 1b-d**). The property enhancement can be attributed to the synergistic effects of the jammed micelle structure and multiple hydrogen bonds between the micelles. These features suppressed macroscopic flow deformation and polymer chain slippage during tensile testing. Furthermore, the hydrogen-bonded micellar ion gel exhibited rapid self-healing behavior at room temperature without any external stimuli. When the cut surfaces of the two cut ion gel pieces were recontacted, the damage was spontaneously repaired within a few hours at room temperature (**Figure 1e**). The self-healing efficiency was quantitatively evaluated through uniaxial tensile testing, and the stress–strain curve recovered to almost the same level as that of the pristine ion gel after 3 h (**Figure 1f**). In this ion gel, the hydrogen bonds between the micelles are preferentially broken upon mechanical damage. Therefore, it is assumed that hydrogen bonds between block copolymer micelles are reformed at the cut surface during reattachment, resulting in rapid self-healing. To demonstrate that the electrochemical properties remain unchanged before and after the repair, we examined the cyclic voltammogram (CV) characteristics and confirmed that there were no changes in the CV profiles. (**Figure 1g**).

Interestingly, the mechanical properties of ion gels are significantly affected not only by the polymer structure but also by subtle differences in the cation and anion structures of the IL. We fabricated ion gels by combining various ILs with the PS-*b*-P(DMAAm-*r*-AAc) diblock copolymer to study the effect of IL structure on the viscoelastic properties of the ion gels (**Figure 2a**).[41] In the presence of 1-ethyl-2,3-dimethylimidazolium ([C_2dmim]) cations, in which a C2 proton with a strong hydrogen-bond-donating ability is methyl-capped, the ion gel became cloudy and brittle, and its elastic modulus increased significantly (**Figure 2b**). Consequently, no self-healing ability was observed in the PS-*b*-P(DMAAm-*r*-AAc)/[C_2dmim][TFSI] ion gel. This effect may be attributed to the lower hydrogen-bond-donating ability of the [C_2dmim] cation compared to the [C_2mim] cation. Thus, the [C_2dmim] cation forms weaker hydrogen bonding with the polymer chain, and very strong hydrogen bonds between the polymer chains themselves are formed. This leads to macroscopic phase separation, causing the ion gel to become cloudy and brittle characteristics. On the other hand, when methyl phosphonate ([MP]) anions, with strong hydrogen-bond-accepting properties, were used as a replacement of [TFSI] anions, the storage modulus of the ion gel decreased significantly. It should be noted that the results of small-angle X-ray scattering measurements suggest that, regardless of the IL used, the ion gels exhibit a microphase-separated structure with comparable micelle sizes.[41] Therefore, the differences in the mechanical properties of the ion gels are likely due to interactions between the hydrogen bonding block and the IL, rather than changes in the compatibility between the PS block and the IL. Fourier-transform infrared (FT-IR) spectroscopy results revealed that the peak shift of the carbonyl group stretching vibration, corresponding to the hydrogen bond between DMAAm and AAc, disappears in the presence of [MP] anions (**Figure 2c**). This indicates that the hydrogen bonding between the [MP] anion and AAc becomes dominant, thereby weakening the hydrogen bonding between the polymer chains and decreasing the storage modulus of the ion gel. Furthermore, the apparent activation energy of each ion gel with a different IL structure was calculated from the Arrhenius plot of the shift factor of the viscoelastic master curve (**Figure 2d**). The activation energy of the ion gel containing [C_2dmim][TFSI] significantly increased, whereas that of the ion gel containing [C_2mim][MP] decreased. These results suggest that controlling competitive hydrogen bonding between cations, anions, and polymer chains is crucial for obtaining the desired mechanical properties, including self-healing ability.

2.2 Self-healing ion gels achieved through physical approaches

Sufficient studies on realizing self-healing functions for polymer materials by using non-covalent or dynamic covalent bonds have been reported. However, the exploration of self-healing polymer materials that utilize physical approaches, such as entanglement between polymer chains or polymer elasticity, has been limited. Yamaguchi et al. conducted pioneering research on controlling the chemical crosslink density of hydrogels near the sol–gel transition point.[42] This approach achieved self-healing functionality through the entanglement of dangling chains. However, the mechanical strength of the hydrogel had to be compromised because of the need to control the crosslink density near the sol–gel transition point. While abundant physical chain entanglement enhances the mechanical strength, it is expected to reduce the self-healing function simultaneously owing to the longer relaxation time associated with the chain entanglement. Therefore, addressing the tradeoff between mechanical strength and self-healing ability is also a significant challenge in self-healing polymeric materials obtained through physical approaches. Recently, we developed an ultrahigh-molecular-weight (UHMW) ion gel formed through the physical entanglement of poly(methyl methacrylate) (PMMA) polymers. The molecular weight of PMMA exceeded 10^6 Da, and it exhibited excellent mechanical strength and self-healing ability (**Figure 3a**).[43] An important finding in the fabrication of UHMW ion gels is that the radical polymerization of methacrylate monomers in the IL at very low initiator concentrations results in UHMW polymers with nearly 100% monomer conversion (**Figure 3b**). In contrast, when using the conventional organic solvent toluene, the monomer conversion decreased significantly at low initiator concentrations, and UHMW polymers could not be produced. Previous experimental and computational investigations into radical polymerization in ILs suggested that the rate constant of propagation (k_p) is enhanced due to a decrease in activation energy caused by IL-radical interactions.[44, 45] In addition, our present study, which compared viscosity-tuned toluene and ILs as polymerization media, revealed that the effect of solvent viscosity—potentially slowing down the termination reaction of growing polymers—on molecular weight was not significant. This suggests that the enhancement of k_p is the dominant factor in the formation of UHMW polymers in ILs. Furthermore, the polydispersity index (PDI) of the obtained UHMW polymers was below 2.0, which is significantly lower than that of high molecular weight polymers produced as a result of a decreased termination rate due to high viscosity, a phenomenon well-known as the Trommsdorff effect.[46] The relatively low PDI in this study could be attributed to the enhanced k_p and the significantly low concentration of radicals under these polymerization conditions, which might reduce the influence of the termination reaction. Consequently, we achieved a simple one-step preparation of ion gels formed solely by the physical entanglement of UHMW polymers, without the need for chemical crosslinking agents. Rheological measurements revealed that the UHMW ion gels maintained their solid-like integrity even at high temperatures (**Figure 3c**). In addition, the UHMW ion gels exhibited higher mechanical strength compared to conventional ion gels with chemical crosslinks (**Figure 3d**). Moreover, because no chemical crosslinking agent was used, the UHMW ion gel could be recycled through hot pressing while maintaining its mechanical strength (**Figure 3e**). Despite being formed by the entanglement of UHMW polymers with very long relaxation times, the UHMW ion gels exhibited rapid self-healing at room temperature (**Figure 3f**). When the cut ion-gel pieces were reattached and subjected to tensile testing, the mechanical strength was restored to a level comparable to that of the pristine sample, as indicated by the stress–strain curve, after 6 hours (**Figure 3g**). Interestingly, when a waiting time between cutting and reattaching the cut gel pieces was allowed, the self-healing efficiency decreased with increasing the waiting time (**Figure 3h**). This phenomenon has also been observed in self-healing polymers based on supramolecular interactions.[47, 48] In the supramolecular system, this phenomenon is explained by the abundance of free non-covalent functional groups that do not form interfacial bonding pairs immediately after cleavage. In the UHMW ion gels, the abundant unentangled polymer chains at the cut interface immediately after cleavage would influence the rapid self-healing properties. Similar to the thermal welding process in glassy polymers, where mechanical recovery occurs more quickly than structural equilibration at the interface,[49] we believe that in UHMW ion gels, structural relaxation of chain entanglement does not fully occur at the interface.The rapid self-healing function might be attributed to the recovery of the entanglement density, which maintains the mechanical strength under tensile test conditions.

In addition, similar to the self-healing of the hydrogen bonded micellar ion gels described in the previous section , subtle differences in the chemical structure of the polymers and the cation–anion structure of the ILs significantly affect the viscoelastic and mechanical properties as well as self-healing performance (**Figure 4a**).[50] For example, the UHMW ion gels containing [C_2mim][TFSI] and [C_{12}mim][TFSI], containing imidazolium cations with different alkyl chain lengths, exhibited similar mechanical strengths in their pristine state. However, their stress–strain curves differed significantly after healing, indicating differences in healing efficiency (**Figure 4b**). All-atom molecular dynamics (MD) simulations of a model oligomer and an IL confirmed the equilibrium conformation of the oligomer and its solvation structure with cations and anions. These simulations revealed that the polymer–IL combination with high healing efficiency had a larger radius of gyration. Additionally, the probability of polymer chains being close to each other was higher in these combinations (**Figure 4c**). This suggests that the microscopic solvation structure and polymer conformation significantly influence the self-healing process. Understanding these detailed mechanisms of the self-healing phenomenon in UHMW ion gels and achieving an even higher level of both mechanical strength and self-healing properties are important challenges to address in the future.

3. Application of functional gel electrolytes in next-generation Li secondary batteries

With the advent of the Internet of Things, the widespread use of electric vehicles, and the promotion of renewable energy to create a low-carbon society, the role of Li secondary batteries is becoming more critical. Li metal is considered as the very promising anode material owing to its very high theoretical capacity and lowest working potential. These features make it a very promising anode material for next-generation high energy density Li secondary batteries.[51-53] However, the high reactivity of Li can lead to the growth of Li dendrites and the formation of dead Li during charging and discharging. These issues raise concerns about safety and battery life. Consequently, Li metal anodes are not yet widely used. To address these challenges, significant efforts have been made to improve the cycling stability of Li metal anodes in recent years. Attempts have been made to actively control the dissolution–deposition process of Li metal anodes by developing new electrolytes,[54-59] functional separators,[60-65] and artificial interphases.[66-71] Recently, there has been considerable interest in the use of artificial interphases for Li metal anodes. Notably, the suppression of Li dendrites and dead Li by polymeric materials with mechanical functions such as self-healing and high toughness has attracted great attention. [72-74]

3.1 Development of robust gel electrolytes for Li metal anodes

Recently, we developed an extremely tough and highly stretchable gel electrolyte by regulating the competitive hydrogen bonding between a highly concentrated electrolyte and a hydrogen-bonded polymer.[75] **Figure 5a** shows the chemical structures of the hydrogen-bonded polymer and an electrolyte solution used to form the gel electrolyte. The electrolyte was an equimolar mixture of tetraglyme (G4) solvent and lithium bis(fluorosulfonyl)imide (LiFSI) ([Li(G4)][FSI]), while the hydrogen-bonded polymer was a combination of methacrylic acid (MAAc) and *N*-methylmethacrylamide (NMMAm). This type of concentrated electrolyte is known as a solvated ionic liquid (SIL). Watanabe et al. reported that SILs exhibit unique physicochemical properties similar to those of ILs, such as high thermal and electrochemical stabilities, owing to the presence of few free solvent molecules in the electrolyte.[76, 77] It is generally known that the FSI anion offers better cycling performance for Li metal anodes compared to the TFSI anion.[78] In SILs, [Li(G4)][FSI] has been reported to form a more stable solid-electrolyte interphase between the Li metal and the electrolyte compared to [Li(G4)][TFSI].[79] Therefore, in this study, we developed a gel electrolyte consisting of [Li(G4)][FSI] and a hydrogen bonding polymer. We utilized the hydrogen bonding between methacrylic acid (MAAc) and *N*-methylmethacrylamide (NMMAm) in [Li(G4)][FSI] to prepare a very tough and highly stretchable gel electrolyte. The key points in the development of gel electrolytes are as follows: (1) optimization of the chemical structure and composition of the hydrogen-bonded polymers and (2) the importance of the composition of the electrolyte solution in the gel electrolyte. **Figure 5b** shows the stress–strain curve of a gel electrolyte consisting of the same hydrogen-bonded polymer and a LiFSI/G4 electrolyte with different Li salt concentrations. Notably, the mechanical strength of the gel electrolyte increased as the Li salt concentration increased, and the best mechanical properties were observed at equimolar concentrations of G4 and LiFSI (LiFSI concentration = 3.2 M). This would be because the number of solvent molecules interacting with Li ions increases as the concentration of the Li salt increases, and the ratio of free solvent molecules interfering with hydrogen bonding between the polymer chains decreases (**Figure 5c**). FT-IR spectroscopy of the gel electrolytes and MD simulations of the model molecules confirmed that at high Li salt concentrations, hydrogen bonds between solvent molecules and polymers were reduced, while strong hydrogen bonds formed between the polymers (**Figure 5d and e**). Based on this concept of regulating competitive hydrogen bonding between the electrolyte and the polymer chain, we fabricated a polymer gel electrolyte with exceptionally high mechanical toughness (~ 16 MJ/m^3), one of the highest reported for polymer gel electrolytes (**Figure 5f**).

3.2 Application of gel electrolytes as artificial interphases of Li metal anodes

The developed tough hydrogen-bonded gel electrolyte was coated onto a Li metal electrode through spin coating to form an artificial protective film. Then, its effect on the performance of Li metal batteries was investigated. Scanning electron microscopy (SEM) and energy dispersive spectroscopy (EDS) revealed that a uniform gel electrolyte layer of approximately 300 nm thickness was coated on the Li metal (**Figure 6a and b**). To verify the effect of the artificial coating on the Li dissolution and deposition processes, long-term cycling tests of Li dissolution and deposition were conducted using a Li-symmetric cell configuration. We found that the cycling performance was significantly improved by introducing a protective gel layer (**Figure 6c**). Without the protective gel layer, short circuits occurred after approximately 200 h, whereas with the protective gel layer, a long cycle time of over 1000 h was possible. SEM observations of the surface of the Li metal anode with a protective coating after 20 cycles confirmed that the Li metal anode was covered with a smooth gel electrolyte film, even after cycling (**Figure 6d**). However, when gel electrolytes with low mechanical strength were coated, the improvement in cycling performance was minimal. This suggests that the tough and strong mechanical properties of the gel electrolyte contribute to the uniform dissolution–deposition process of the Li metal. However, various factors of the protective film are thought to affect the dissolution–deposition process of the Li metal anode.[51, 66] Therefore, understanding the detailed mechanism and identifying the contributing factors that improve cycling performance are key issues to address in the future. Furthermore, a full cell consisting of a $LiNi_{0.6}Co_{0.2}Mn_{0.2}O_2$ (NCM622) cathode, a high-energy cathode material, and a Li metal anode was fabricated, and the effect of the artificial protective coating of the gel electrolyte on battery performance was verified. When a Li metal anode without a protective gel coating was used, a significant decrease in capacity and Coulombic efficiency was observed, and the capacity retention after 50 cycles was approximately 80%. On the other hand, when the gel electrolyte was coated as a protective film, stable cycling performance with high Coulombic efficiency was observed, and a high capacity retention of 87% was achieved after 100 cycles (**Figure 6e and f**). These results confirm the significant improvement in cycle performance due to the introduction of the artificial protective coating of tough gel electrolytes, even in the full-cell configuration.

3.3 Future challenges associated with the usage of Li metal anode

The application of polymeric materials as artificial protective coatings is expected to be promising strategy for the use of Li metal electrodes in next-generation Li secondary batteries. The tough and stretchable features of gel electrolytes are also expected to make them applicable in flexible batteries, which have attracted significant attention in recent years for IoT devices.[80, 81] However, the research remains in its early stages, and several challenges and issues need to be addressed before these solutions can be applied to practical battery systems. Optimization of the thickness of the protective film and applicability to other electrolyte systems must be considered. It is also essential to evaluate the performance improvement when using a lean amount of electrolyte, as this reflects a more practical condition for commercial batteries.[82] Additionally, the integration of suitable cathode materials is crucial, as it significantly affects the overall performance and efficiency of the battery system. In addition to material development, observation of the degradation behavior of battery cells over time is also very important for the practical use of Li metal anodes. Observing the interior of cells through nondestructive characterization, including operando measurements, is considered an important technique for verifying the long-term behavior of Li-metal batteries. Recently, we analyzed the inside of a Li symmetric cell without disassembling the cell after cycling using nondestructive X-ray computed tomography (X-ray CT) measurements.[83] X-ray CT analysis of slice images successfully revealed differences in the morphological evolution of Li metal anodes during dissolution and deposition cycles between conventional and highly concentrated electrolytes (**Figure 7a-c**). Utilizing this advanced measurement technique can significantly aid in the development of materials that support more reversible Li dissolution and deposition behavior.

4. Conclusion

In this review, we discuss our recent research on gel electrolytes with mechanical functions, such as self-healing ability and high mechanical strength. Moreover, the review discusses the application of functional gel electrolytes to Li metal batteries. Polymeric materials with self-healing properties have recently attracted attention as innovative materials that can enhance the durability by actively repairing mechanical damage. In this review, self-healing ion gel electrolytes obtained using physical and chemical approaches are discussed. Additionally, we present the fabrication of a Li - conductive gel electrolyte with exceptional mechanical toughness, made from a highly concentrated Li salt electrolyte and a hydrogen-bonded polymer. In both gel electrolytes, not only the polymer structure, but also the electrolyte composition (cation, anion, and solvent molecules) had a significant influence on the mechanical functions, which is a major feature of gel electrolytes. Understanding and controlling the interaction between the polymer and electrolyte is crucial for realizing gel electrolytes with better functionality in the future.

In addition, it was found that the developed gel electrolyte acts as a protective film for Li metal anodes and enhances the cycling performance of Li metal batteries. In the future, it will be desirable to develop polymer gel electrolytes that enhance the practical use of Li metal anodes by identifying the key factors in gel electrolytes that affect the cycling performance.

Acknowledgments

The author is sincerely grateful to all his colleagues for their collaboration and encouragement in this work. This work was financially supported by JSPS KAKENHI (23K26409), JST PRESTO program (JPMJPR2196), COI-NEXT (JPMJPF2016), and Green Technologies of Excellence (GteX) Program (JPMJGX23S3).

References

1. Zhang Y, Jeong CK, Wang J, Chen X, Choi KH, Chen LQ, et al. Hydrogel ionic diodes toward harvesting ultralow-frequency mechanical energy. Adv Mater. 2021;33:2103056.
2. Wang H, Wang Z, Yang J, Xu C, Zhang Q, Peng Z. Ionic gels and their applications in stretchable electronics. Macromol Rapid Commun. 2018;39:1800246.
3. Shi Y, Zhang J, Pan L, Shi Y, Yu G. Energy gels: A bio-inspired material platform for advanced energy applications. Nano Today. 2016;11:738–762.
4. Cheng X, Pan J, Zhao Y, Liao M, Peng H. Gel polymer electrolytes for electrochemical energy storage. Adv Energy Mater. 2018;8:1702184.
5. Wang Z, Li H, Tang Z, Liu Z, Ruan Z, Ma L, et al. Hydrogel electrolytes for flexible aqueous energy storage devices. Adv Funct Mater. 2018;28:1804560.
6. Chen T, Kong W, Zhang Z, Wang L, Hu Y, Zhu G, et al. Ionic liquid-immobilized polymer gel electrolyte with self-healing capability, high ionic conductivity and heat resistance for dendrite-free lithium metal batteries. Nano Energy. 2018;54:17–25.
7. Kamio E, Yasui T, Iida Y, Gong JP, Matsuyama H. Inorganic/organic double-network gels containing ionic liquids. Adv Mater. 2017;29:1704118.
8. Wang M, Zhang P, Shamsi M, Thelen JL, Qian W, Truong VK, et al. Tough and stretchable ionogels by in situ phase separation. Nat Mater. 2022;21:359-365.
9. Zhao Y, Zhang Y, Sun H, Dong X, Cao J, Wang L, et al. A self-healing aqueous lithium-ion battery. Angew Chem Int Ed. 2016;55:14384–14388.
10. Wang C, Li R, Chen P, Fu Y, Ma X, Shen T, et al. Highly stretchable, non-flammable and notch-insensitive intrinsic self-healing solid-state polymer electrolyte for stable and safe flexible lithium batteries. J Mater Chem A. 2021;9:4758–4769.
11. Wu H, Cao Y, Su H, Wang C. Tough gel electrolyte using double polymer network design for the safe, stable cycling of lithium metal anode. Angew Chem Int Ed. 2018;57:1361–1365.
12. Hashimoto K, Tatara R, Ueno K, Dokko K, Watanabe M. Design of polymer network and Li + solvation enables thermally and oxidatively stable, mechanically reliable, and highly conductive polymer gel electrolyte for lithium batteries. J Electrochem Soc. 2021;168:090538.
13. Angell CA, Ansari Y, Zhao Z. Ionic liquids: past, present and future. Faraday Discuss. 2012;154:9–27.
14. Ueno K, Tokuda H, Watanabe M. Ionicity in ionic liquids: correlation with ionic structure and physicochemical properties. Phys Chem Chem Phys. 2010;12:1649–1658.
15. MacFarlane DR, Tachikawa N, Forsyth M, Pringle JM, Howlett PC, Elliott GD, et al.

Energy applications of ionic liquids. Energy Environ Sci. 2014;7:232–250.
16. Hayes R, Warr GG, Atkin R. Structure and nanostructure in ionic liquids. Chem Rev. 2015;115:6357–6426.
17. Ohno H, Yoshizawa-Fujita M, Kohno Y. Functional design of ionic liquids: Unprecedented liquids that contribute to energy technology, bioscience, and materials sciences. Bull Chem Soc Jpn. 2019;92:852-868.
18. Tamate R, Hashimoto K, Ueki T, Watanabe M. Block copolymer self-assembly in ionic liquids. Phys Chem Chem Phys. 2018;20:25123–25139.
19. Wang M, Hu J, Dickey MD. Tough ionogels: synthesis, toughening mechanisms, and mechanical properties─a perspective. JACS Au. 2022;2: 2645–2657.
20. MacFarlane DR, Forsyth M, Howlett PC, Kar M, Passerini S, Pringle JM, et al. Ionic liquids and their solid-state analogues as materials for energy generation and storage. Nat Rev Mater. 2016;1:15005.
21. Yan CC, Li WZ, Liu ZY, Zheng SJ, Hu Y, Zhou YJ, et al. Ionogels: preparation, properties and applications. Adv Funct Materials. 2024;34:2314408.
22. Cho KG, An S, Cho DH, Kim JH, Nam J, Kim M, et al. Block copolymer-based supramolecular ionogels for accurate on-skin motion monitoring. Adv Funct Mater. 2021;31:2102386.
23. Chen N, Zhang H, Li L, Chen R, Guo S. Ionogel electrolytes for high-performance lithium batteries: a review. Adv Energy Mater. 2018;8:1702675.
24. Wu DY, Meure S, Solomon D. Self-healing polymeric materials: a review of recent developments. Prog Polym Sci. 2008;33:479–522.
25. Yang Y, Urban MW. Self-healing polymeric materials. Chem Soc Rev. 2013;42:7446–7467.
26. Kang J, Tok JBH, Bao Z. Self-healing soft electronics. Nat Electron. 2019;2:144–150.
27. Maeda T, Otsuka H, Takahara A. Dynamic covalent polymers: Reorganizable polymers with dynamic covalent bonds. Prog Polym Sci. 2009;34:581–604.
28. Wang S, Urban MW. Self-healing polymers. Nat Rev Mater. 2020;5:562–583.
29. Li B, Cao P-F, Saito T, Sokolov AP. Intrinsically self-healing polymers: from mechanistic insight to current challenges. Chem Rev. 2023;123:701–735.
30. Tamate R, Watanabe M. Recent progress in self-healable ion gels. Sci Technol Adv Mater. 2020;21:388–401.
31. Tamate R. Healable soft materials based on ionic liquids and block copolymer self-assembly. Polym J. 2021;53:789–798.
32. Tamate R, Ueki T. Adaptive ion-gel: stimuli-responsive, and self-healing ion gels. Chem Rec. 2023;23:e202300043.

33. Cao Y, Morrissey TG, Acome E, Allec SI, Wong BM, Keplinger C, et al. A transparent, self-healing, highly stretchable ionic conductor. Adv Mater. 2017;29:1605099.
34. Saruwatari A, Tamate R, Kokubo H, Watanabe M. Photohealable ion gels based on the reversible dimerisation of anthracene. Chem Commun. 2018;54:13371–13374.
35. Xu L, Huang Z, Deng Z, Du Z, Sun TL, Guo ZH, et al. A transparent, highly stretchable, solvent-resistant, recyclable multifunctional ionogel with underwater self-healing and adhesion for reliable strain sensors. Adv Mater. 2021;33:2105306.
36. Yang L, Sun L, Huang H, Zhu W, Wang Y, Wu Z, et al. Mechanically robust and room temperature self-healing ionogel based on ionic liquid inhibited reversible reaction of disulfide bonds. Adv Sci. 2023;10:2207527.
37. Kim YM, Kwon JH, Kim S, Choi UH, Moon HC. Ion-cluster-mediated ultrafast self-healable ionoconductors for reconfigurable electronics. Nat Commun. 2022;13:3769.
38. Kim S, Yeo J, Kim SJ, Park S, Cho KG, Paeng K, et al. Photopatternable and self-healable ionogels for organic thin-film transistors. Organic Electronics. 2023;122:106895.
39. Yu Z, Wu P. Underwater communication and optical camouflage ionogels. Adv Mater. 2021;33:2008479.
40. Tamate R, Hashimoto K, Horii T, Hirasawa M, Li X, Shibayama M, et al. Self-healing micellar ion gels based on multiple hydrogen bonding. Adv Mater. 2018;30:1802792.
41. Tamate R, Hashimoto K, Li X, Shibayama M, Watanabe M. Effect of ionic liquid structure on viscoelastic behavior of hydrogen-bonded micellar ion gels. Polymer. 2019;178:121694.
42. Yamaguchi M, Ono S, Okamoto K. Interdiffusion of dangling chains in weak gel and its application to self-repairing material. Mater Sci Eng B. 2009;162:189–194.
43. Kamiyama Y, Tamate R, Hiroi T, Samitsu S, Fujii K, Ueki T. Highly stretchable and self-healable polymer gels from physical entanglements of ultrahigh–molecular weight polymers. Sci Adv. 2022;8:eadd0226.
44. Harrisson S, Mackenzie SR, Haddleton DM. Unprecedented solvent-induced acceleration of free-radical propagation of methyl methacrylate in ionic liquids. Chem Commun. 2002:2850–2851.
45. Low K, Wylie L, Scarborough DLA, Izgorodina EI. Is it possible to control kinetic rates of radical polymerisation in ionic liquids? Chem Commun. 2018;54:11226–11243.
46. Suzuki Y, Shinagawa Y, Kato E, Mishima R, Fukao K, Matsumoto A. Polymerization-induced vitrification and kinetic heterogenization at the onset of the Trommsdorff effect. Macromolecules. 2021;54:3293–3303.

47. Cordier P, Tournilhac F, Soulié-Ziakovic C, Leibler L. Self-healing and thermoreversible rubber from supramolecular assembly. Nature. 2008;451:977–980.
48. Stukalin EB, Cai LH, Kumar NA, Leibler L, Rubinstein M. Self-healing of unentangled polymer networks with reversible bonds. Macromolecules. 2013;46:7525–7541.
49. Ge T, Grest GS, Robbins MO. Tensile fracture of welded polymer interfaces: miscibility, entanglements, and crazing. Macromolecules. 2014;47:6982–6989.
50. Kamiyama Y, Tamate R, Fujii K, Ueki T. Controlling mechanical properties of ultrahigh molecular weight ion gels by chemical structure of ionic liquids and monomers. Soft Matter. 2022;18:8582–8590.
51. Tikekar MD, Choudhury S, Tu Z, Archer LA. Design principles for electrolytes and interfaces for stable lithium-metal batteries. Nat Energy. 2016;1:16114.
52. Guo Y, Li H, Zhai T. Reviving lithium-metal anodes for next-generation high-energy batteries. Adv Mater. 2017;29:1700007.
53. Cheng X-B, Zhang R, Zhao CZ, Zhang Q. Toward safe lithium metal anode in rechargeable batteries: a review. Chem Rev. 2017;117:10403–10473.
54. Watanabe M, Dokko K, Ueno K, Thomas ML. From ionic liquids to solvate ionic liquids: challenges and opportunities for next generation battery electrolytes. Bull Chem Soc Jpn. 2018;91:1660–1682.
55. Yamada Y, Yamada A. Review—superconcentrated electrolytes for lithium batteries. J Electrochem Soc. 2015;162:A2406–A2423.
56. Xiao P, Yun X, Chen Y, Guo X, Gao P, Zhou G, et al. Insights into the solvation chemistry in liquid electrolytes for lithium-based rechargeable batteries. Chem Soc Rev. 2023;52:5255–5316.
57. Yoshida K, Nakamura M, Kazue Y, Tachikawa N, Tsuzuki S, Seki S, et al. Oxidative-stability enhancement and charge transport mechanism in glyme–lithium salt equimolar complexes. J Am Chem Soc. 2011;133:13121–13129.
58. Yamada Y, Furukawa K, Sodeyama K, Kikuchi K, Yaegashi M, Tateyama Y, et al. Unusual stability of acetonitrile-based superconcentrated electrolytes for fast-charging lithium-ion batteries. J Am Chem Soc. 2014;136:5039–5046.
59. Ciurduc DE, Boaretto N, Fernández-Blázquez JP, Marcilla R. Development of high performing polymer electrolytes based on superconcentrated solutions. J Power Sources. 2021;506:230220.
60. Hao Z, Zhao Q, Tang J, Zhang Q, Liu J, Jin Y, et al. Functional separators towards the suppression of lithium dendrites for rechargeable high-energy batteries. Mater Horiz. 2021;8:12–32.

61. Huang B, Luo J, Xu B, Li Z, Li Y, Che Y, et al. Surface coating on a separator with a reductive solid Li-ion conductor for dendrite-free Li-metal batteries. ACS Appl Energy Mater. 2021;4:8621–8628.
62. Poungsripong P, Tamate R, Ono M, Sakaushi K, Ue M. Fabrication of single-ion conducting polymer-coated separators and their application in nonaqueous Li-O2 batteries. Polym J. 2021;53:549–556.
63. Shomura R, Tamate R, Matsuda S. Lithium-ion-conducting ceramics-coated separator for stable operation of lithium metal-based rechargeable batteries. Materials 2022;15:322.
64. Ryou MH, Lee DJ, Lee JN, Lee YM, Park JK, Choi JW. Excellent cycle life of lithium-metal anodes in lithium-ion batteries with mussel-inspired polydopamine-coated separators. Adv Energy Mater. 2012;2:645–650.
65. Zhang W, Tu Z, Qian J, Choudhury S, Archer LA, Lu Y. Design principles of functional polymer separators for high-energy, metal-based batteries. Small. 2018;14:1703001.
66. Yu Z, Cui Y, Bao Z. Design principles of artificial solid electrolyte interphases for lithium-metal anodes. Cell Rep Phys Sci. 2020;1:100119.
67. Tu Z, Choudhury S, Zachman MJ, Wei S, Zhang K, Kourkoutis LF, et al. Designing artificial solid-electrolyte interphases for single-ion and high-efficiency transport in batteries. Joule. 2017;1:394–406.
68. Xu R, Zhang XQ, Cheng XB, Peng HJ, Zhao CZ, Yan C, et al. Artificial soft-rigid protective layer for dendrite-free lithium metal anode. Adv Funct Materials. 2018;28:1705838.
69. Yang D, Li J, Yang F, Li J, He L, Zhao H, et al. A rigid-flexible protecting film with surface pits structure for dendrite-free and high-performance lithium metal anode. Nano Lett. 2021;21:7063–7069.
70. Gao Y, Yan Z, Gray JL, He X, Wang D, Chen T, et al. Polymer–inorganic solid–electrolyte interphase for stable lithium metal batteries under lean electrolyte conditions. Nat Mater. 2019;18:384–389.
71. Xu R, Cheng XB, Yan C, Zhang XQ, Xiao Y, Zhao CZ, et al. Artificial interphases for highly stable lithium metal anode. Matter. 2019;1:317–344.
72. Liu K, Pei A, Lee HR, Kong B, Liu N, Lin D, et al. Lithium metal anodes with an adaptive "solid-liquid" interfacial protective layer. J Am Chem Soc. 2017;139:4815–4820.
73. Wang Y, Zanelotti CJ, Wang X, Kerr R, Jin L, Kan WH, et al. Solid-state rigid-rod polymer composite electrolytes with nanocrystalline lithium ion pathways. Nat Mater.

2021;20:1255–1263.
74. Jaumaux P, Liu Q, Zhou D, Xu X, Wang T, Wang Y, et al. Deep-eutectic-solvent-based self-healing polymer electrolyte for safe and long-life lithium-metal batteries. Angew Chem Int Ed Engl. 2020;59:9134–9142.
75. Tamate R, Peng Y, Kamiyama Y, Nishikawa K. Extremely tough, stretchable gel electrolytes with strong interpolymer hydrogen bonding prepared using concentrated electrolytes to stabilize lithium-metal anodes. Adv Mater. 2023;35:2211679.
76. Ueno K, Yoshida K, Tsuchiya M, Tachikawa N, Dokko K, Watanabe M. Glyme–lithium salt equimolar molten mixtures: concentrated solutions or solvate ionic liquids? J Phys Chem B. 2012;116:11323–11331.
77. Mandai T, Yoshida K, Ueno K, Dokko K, Watanabe M. Criteria for solvate ionic liquids. Phys Chem Chem Phys. 2014;16:8761–8772.
78. Shkrob IA, Marin TW, Zhu Y, Abraham DP. Why bis(fluorosulfonyl)imide is a "magic anion" for electrochemistry. J Phys Chem C. 2014;118:19661–19671.
79. Tatara R, Ikeda K, Ueno K, Watanabe M, Dokko K. Solid–electrolyte interphase formation during Li metal deposition in $LiN(SO_2F)_2$-based solvate ionic liquids. J Solid State Electrochem. DOI: 10.1007/s10008-024-05843-4
80. Chang J, Huang Q, Gao Y, Zheng Z. Pathways of developing high-energy-density flexible lithium batteries. Adv Mater. 2021;33:2004419.
81. Kong L, Tang C, Peng HJ, Huang JQ, Zhang Q. Advanced energy materials for flexible batteries in energy storage: a review. SmartMat. 2020;1:e1007
82. Liu J, Bao Z, Cui Y, Dufek EJ, Goodenough JB, Khalifah P, et al. Pathways for practical high-energy long-cycling lithium metal batteries. Nat Energy. 2019;4:180–186.
83. Tamate R, Matsuda S. Asymmetric volume expansion of the lithium metal electrode in symmetric lithium/lithium cells under lean electrolyte and high areal capacity conditions. ACS Appl Energy Mater. 2023;6:573–579.

Titles and legends to figures

Figure 1. (a) Schematic and chemical structures of self-healing ion gels composed of hydrogen bonding and nanophase separation of a diblock copolymer in an IL. (b) Self-standing ability, (c) rheological temperature sweep measurements, and (d) uniaxial tensile tests for PS-*b*-P(DMAAm-*r*-AAc) and P(DMAAm-*r*-AAc) ion gels. (e) Self-healing behavior of the PS-*b*-P(DMAAm-*r*-AAc) ion gel at room temperature. (f) Stress–strain curves of the pristine ion gel and the healed ion gels at different healing times. (g) Cyclic voltammogram of ion gels before cutting and 3 h after healing. Reproduced with permission from Ref. [40]. Copyright 2018 Wiley-VCH.

Figure 2. (a) Schematic of competitive hydrogen bonding in the hydrogen-bonded micellar ion gel network. (b) Temperature sweep measurements of the PS-*b*-P(DMAAm-*r*-AAc) ion gels with different ILs as electrolytes. (c) FT-IR spectra of ion gels with different ILs. (d) Apparent activation energy of each ion gel calculated from an Arrhenius plot of the shift factor of the viscoelastic master curve. Reproduced with permission from Ref. [41]. Copyright 2019 Elsevier.

Figure 3. (a) Photograph and schematic of the UHMW ion gel consisting of entangled UHMW polymers in an IL. (b) Dependence of monomer conversion and number-

averaged molecular weight (M_n) on thermal initiator concentration during the radical polymerization of methyl methacrylate in [C_2mim][TFSI] and toluene. (c) Rheological temperature sweep measurements of composites made from PMMA with varying molecular weights and [C_2mim][TFSI]. (d) Comparison of compressive and tensile test results for the UHMW ion gel and a conventional chemically crosslinked ion gel. (e) Uniaxial tensile tests for the UHMW ion gel, chemically crosslinked ion gel, and the recycled UHMW ion gel, including a photograph of the recycling process. The recycling process was carried out by hot pressing at 130 °C. (f) Photographs of the self-healing behavior of the UHMW ion gel. (g) Stress–strain curves for the pristine UHMW ion gel and healed UHMW ion gels with different healing times at room temperature. (h) Differences in stress–strain curves for healed UHMW ion gels with different waiting times. Reproduced under the terms of the Creative Commons CC BY-NC license from Ref. [43]. Copyright 2022 AAAS.

Figure 4. (a) Chemical structures of monomers, IL cations, and anions constituting UHMW ion gels. (b) Comparison of stress–strain curves of pristine and healed samples of PMMA/[C_2mim][TFSI] and PMMA/[C_{12}mim][TFSI] UHMW ion gels. (c) Comparison of intermolecular radial distribution functions of model oligomers in ILs

obtained from all-atom MD calculations and representative snapshots of two adjacent oligomers. Reproduced with permission from Ref. [50]. Copyright 2022 RSC.

Figure 5. (a) Chemical structures of a hydrogen-bonded polymer and an electrolyte constituting the tough hydrogen-bonded gel electrolytes. (b) Stress–strain curves of the gel electrolytes with different LiFSI salt concentrations. (c) Schematic of the difference in interpolymer hydrogen bonding with electrolytes having conventional and high salt concentrations. (d) FT-IR spectra of the gel electrolytes with conventional and high Li salt concentrations. (e) Differences in pair correlation functions of the hydrogen atom of the donor monomer and the oxygen atom of the acceptor monomer constituting the hydrogen-bonding polymers. The data was obtained by all-atom MD calculations for with conventional and high salt concentration conditions. (f) Uniaxial tensile tests of gel electrolytes. Reproduced with permission from Ref. [75]. Copyright 2023 Wiley-VCH.

Figure 6. (a) Cross-sectional SEM and (b) EDS images of hydrogen-bonded gel electrolytes coated on the Li metal. The red and green colors represent the presence of carbon (C) and oxygen (O) elements. The intense green and red signals in the layer on the Li surface indicate the presence of C and O atoms from the coated gel layer. (c) Differences in dissolution–deposition cycles of a Li/Li symmetric cell with and without

the protective coating of the gel electrolyte. In both Li/Li symmetric cells, the electrolyte layer was a glass microfiber separator soaked with [Li(G4)][FSI] electrolyte. (d) Surface SEM images of pristine Li and the gel-coated Li foil after 20 cycles. Differences in (e) discharge capacity and (f) Coulombic efficiency with and without the gel electrolyte coating in a full cell consisting of a Li anode and an NCM622 cathode. Reproduced with permission from Ref. [75]. Copyright 2023 Wiley-VCH.

Figure 7. (a) Photograph of the setup for X-ray CT measurement of a Li/Li symmetric pouch cell. (b, c) Slice images from nondestructive X-ray CT analysis of Li/Li symmetric cells after 20 cycles with (b) a conventional concentration electrolyte (1 M LiFSI in 1,2-dimethoxyethane (DME)) and (c) a highly concentrated electrolyte (4 M LiFSI in DME). Reproduced with permission from Ref. [83]. Copyright 2023 ACS.

Figures

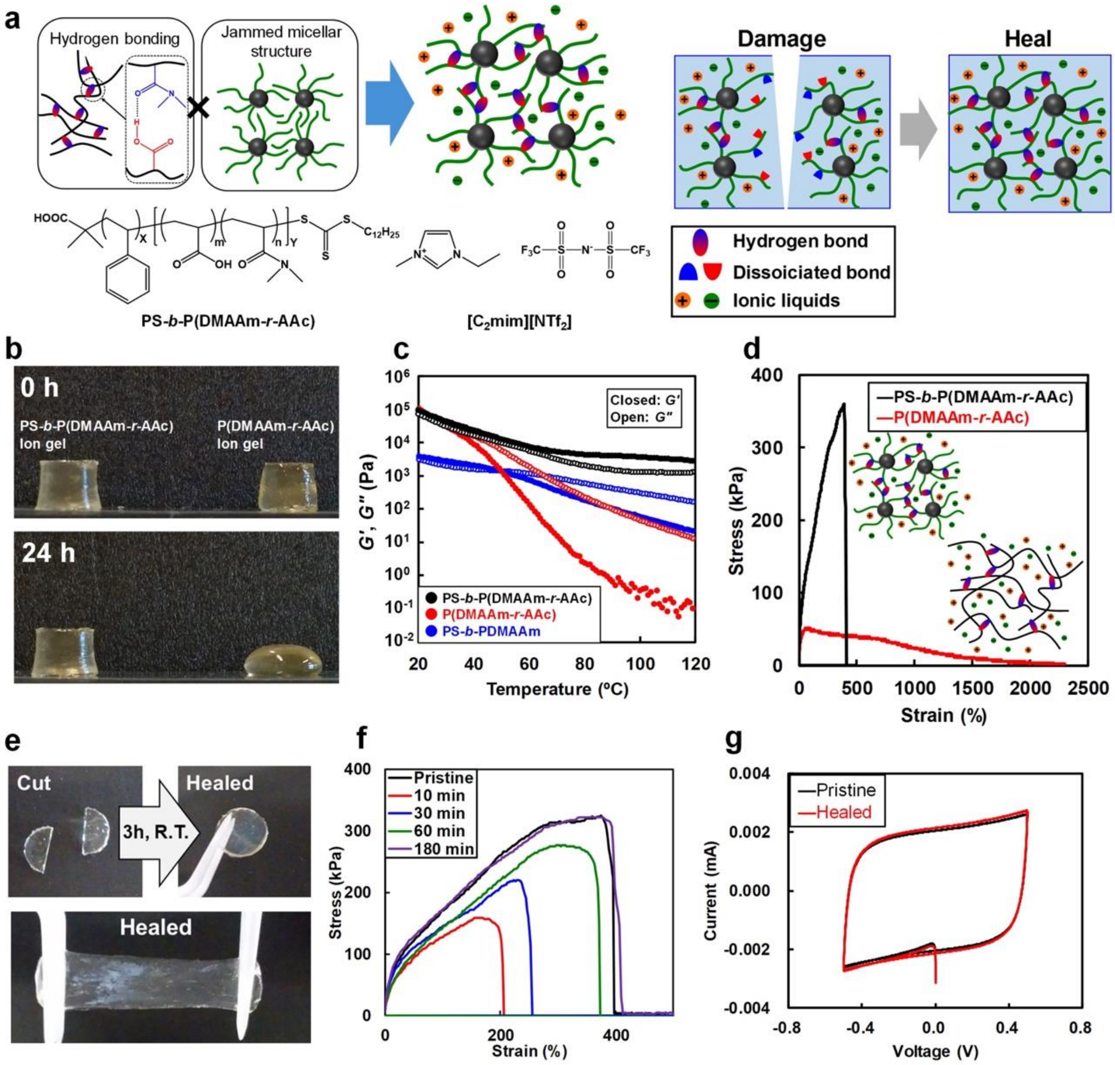

Figure 1.

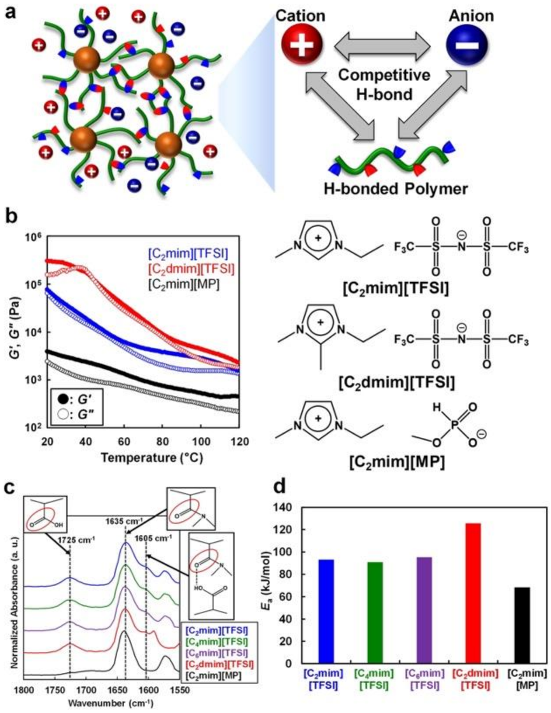
a
Cation
Anion
Competitive
H-bond
H-bonded Polymer
b
[C2mim][TFSI]
[C2dmim][TFSI]
[C2mim][MP]
G′, G″ (Pa)
●: G′
○: G″
Temperature (°C)
c
1725 cm⁻¹
1635 cm⁻¹
1605 cm⁻¹
Normalized Absorbance (a. u.)
Wavenumber (cm⁻¹)
[C2mim][TFSI]
[C4mim][TFSI]
[C6mim][TFSI]
[C2dmim][TFSI]
[C2mim][MP]
d
Ea (kJ/mol)

Figure 2.

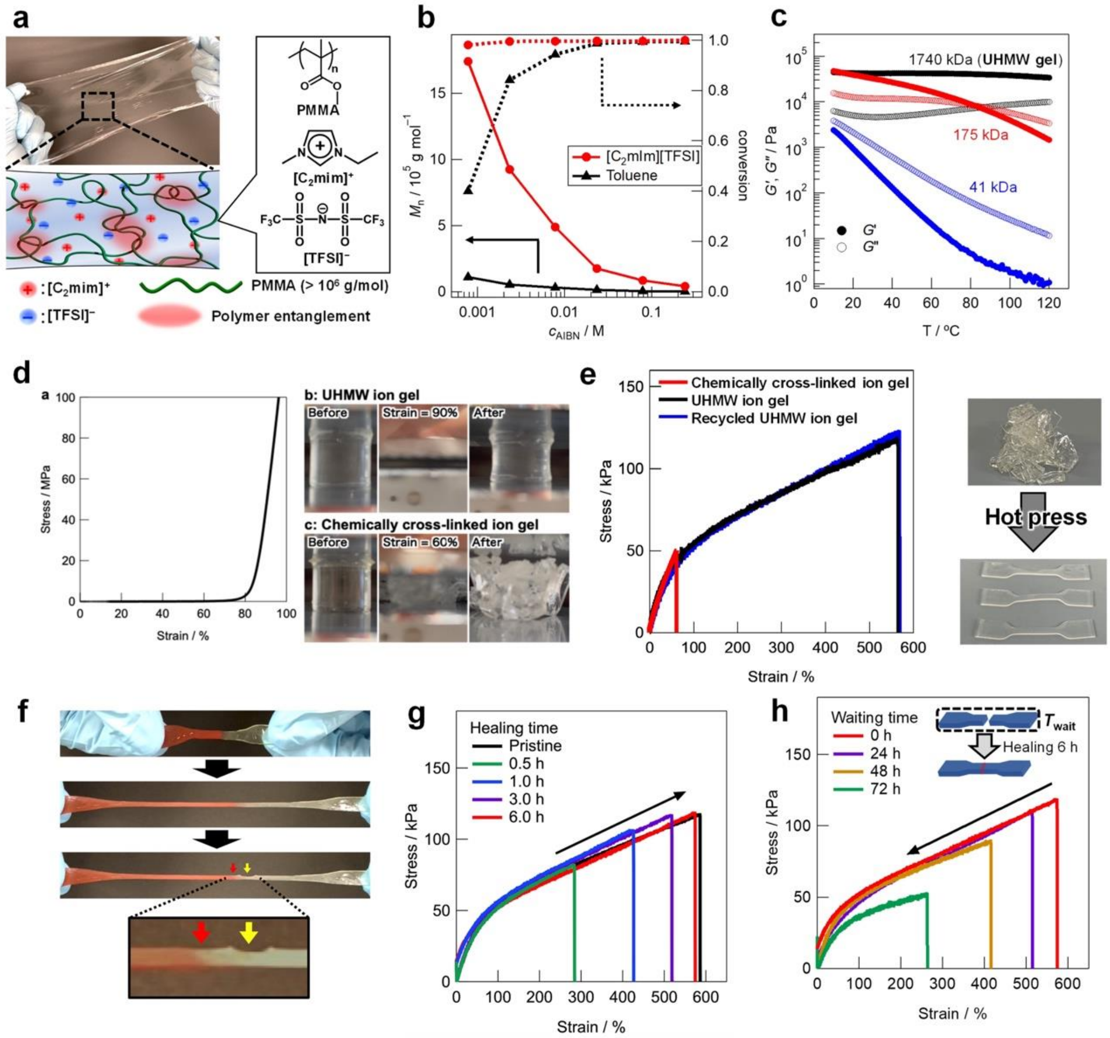

a
PMMA
[C2mim]+
[TFSI]−
: [C2mim]+
: [TFSI]−
PMMA (> 10^6 g/mol)
Polymer entanglement
b
[C2mIm][TFSI]
Toluene
conversion
cAIBN / M
c
1740 kDa (UHMW gel)
175 kDa
41 kDa
G'
G"
T / °C
d
b: UHMW ion gel
Before
Strain = 90%
After
c: Chemically cross-linked ion gel
Strain = 60%
Stress / MPa
Strain / %
e
Chemically cross-linked ion gel
UHMW ion gel
Recycled UHMW ion gel
Stress / kPa
Hot press
f
g
Healing time
Pristine
0.5 h
1.0 h
3.0 h
6.0 h
h
Waiting time
0 h
24 h
48 h
72 h
Healing 6 h

Figure 3.

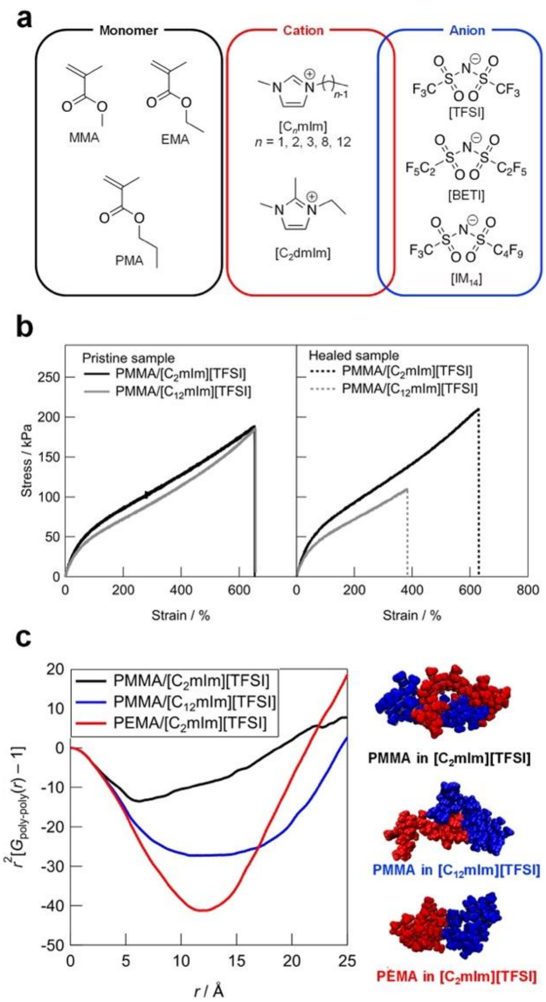
a
Monomer
Cation
Anion
MMA
EMA
PMA
[CnmIm]
n = 1, 2, 3, 8, 12
[C2dmIm]
[TFSI]
[BETI]
[IM14]
b
Pristine sample
PMMA/[C2mIm][TFSI]
PMMA/[C12mIm][TFSI]
Healed sample
PMMA/[C2mIm][TFSI]
PMMA/[C12mIm][TFSI]
Stress / kPa
Strain / %
c
PMMA/[C2mIm][TFSI]
PMMA/[C12mIm][TFSI]
PEMA/[C2mIm][TFSI]
r2[Gpoly-poly(r) − 1]
r / Å
PMMA in [C2mIm][TFSI]
PMMA in [C12mIm][TFSI]
PEMA in [C2mIm][TFSI]

Figure 4.

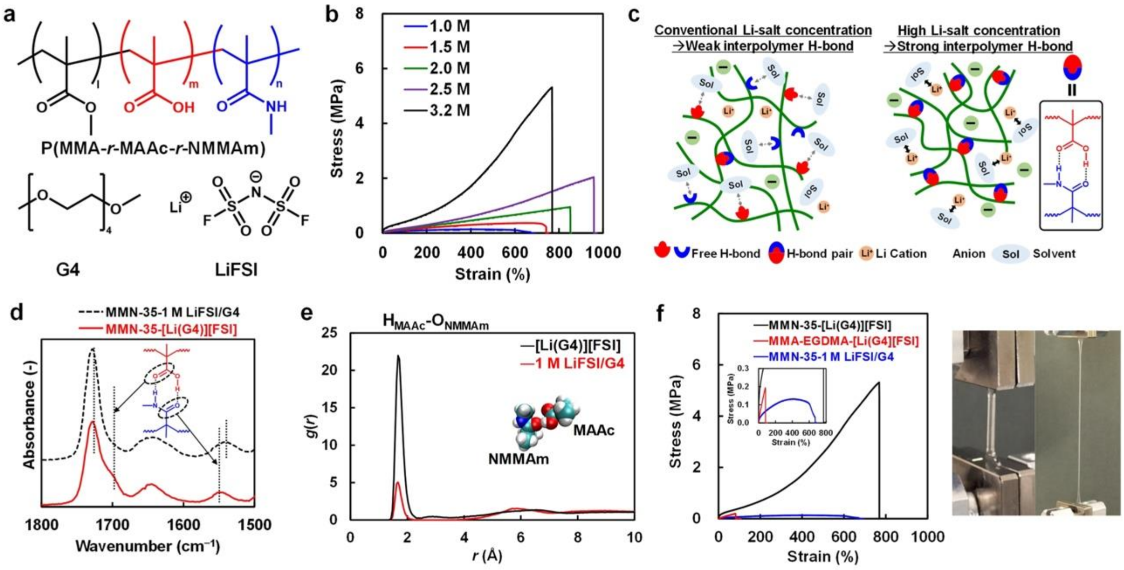

a
P(MMA-r-MAAc-r-NMMAm)
G4
LiFSI
b
1.0 M
1.5 M
2.0 M
2.5 M
3.2 M
Stress (MPa)
Strain (%)
c
Conventional Li-salt concentration →Weak interpolymer H-bond
High Li-salt concentration →Strong interpolymer H-bond
Free H-bond
H-bond pair
Li Cation
Anion
Sol
Solvent
d
MMN-35-1 M LiFSI/G4
MMN-35-[Li(G4)][FSI]
Absorbance (-)
Wavenumber (cm⁻¹)
e
H_MAAc-O_NMMAm
[Li(G4)][FSI]
1 M LiFSI/G4
g(r)
NMMAm
MAAc
r (Å)
f
MMN-35-[Li(G4)][FSI]
MMA-EGDMA-[Li(G4)][FSI]
MMN-35-1 M LiFSI/G4
Stress (MPa)
Strain (%)

Figure 5.

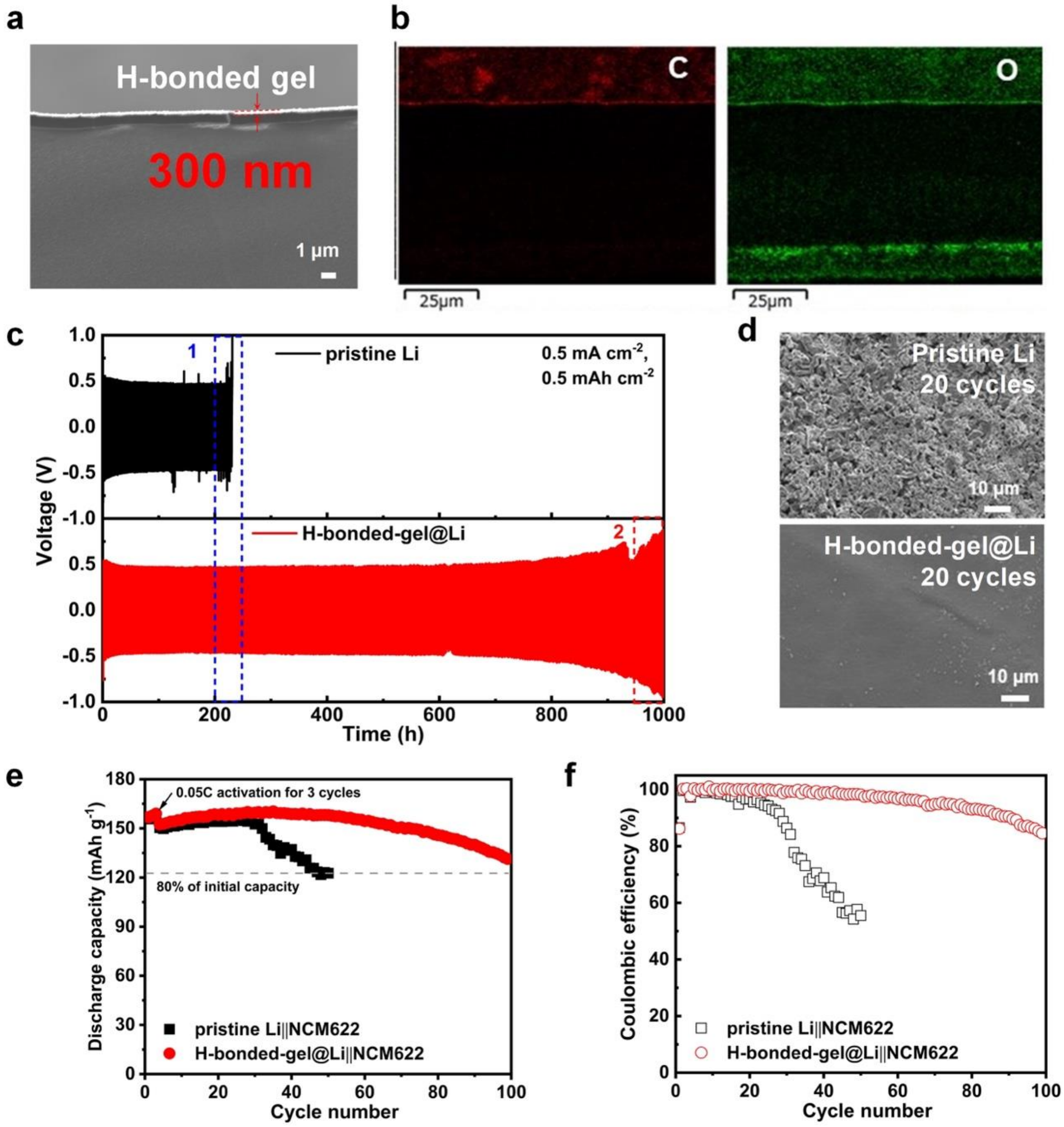
a
H-bonded gel
300 nm
1 µm
b
C
O
25µm
25µm
c
pristine Li
0.5 mA cm-2,
0.5 mAh cm-2
H-bonded-gel@Li
Voltage (V)
Time (h)
d
Pristine Li
20 cycles
10 µm
H-bonded-gel@Li
20 cycles
10 µm
e
0.05C activation for 3 cycles
80% of initial capacity
Discharge capacity (mAh g-1)
pristine Li||NCM622
H-bonded-gel@Li||NCM622
Cycle number
f
Coulombic efficiency (%)
pristine Li||NCM622
H-bonded-gel@Li||NCM622
Cycle number

Figure 6.

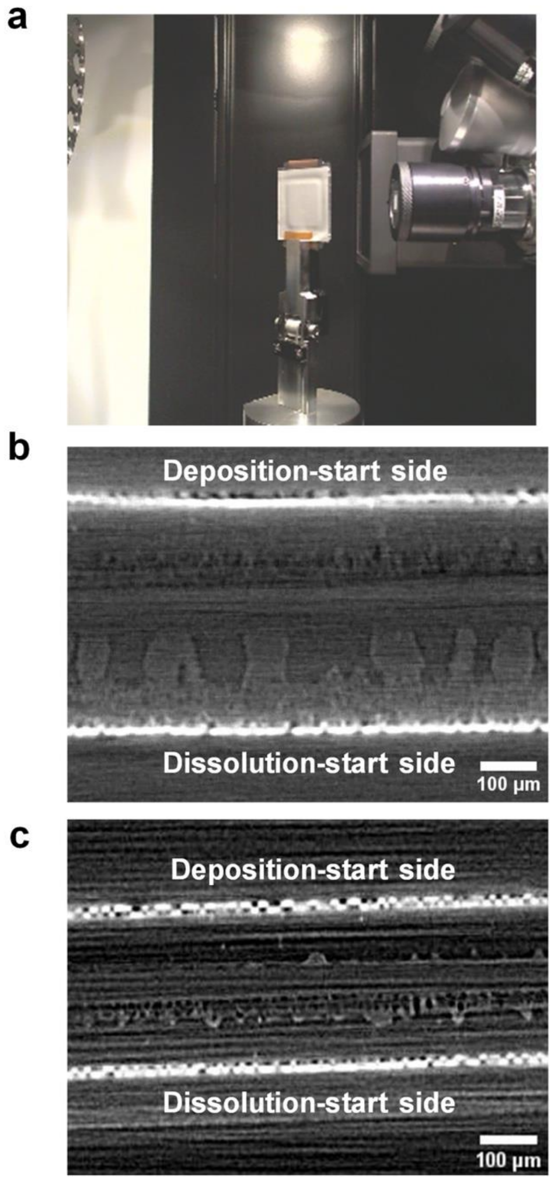
a
b
Deposition-start side
Dissolution-start side
100 µm
c
Deposition-start side
Dissolution-start side
100 µm

Figure 7.

Graphical Abstract

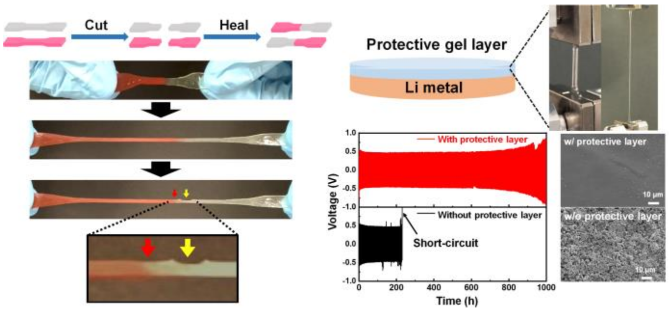

This focus review presents our recent research on enhancing the mechanical properties of gel electrolytes and their application in lithium secondary batteries. It discusses the efforts made to achieve self-healing ion gels, which utilize ionic liquids as the electrolyte solutions. Additionally, the review covers the application of functional gel electrolytes in next-generation lithium secondary batteries. It focuses particularly on improving the cycling performance of lithium metal anodes, which are considered the very promising anode material.